



# All-optical responsive azo-doped liquid crystal laser protection filter

ETHAN I. L. JULL\* AND HELEN F. GLEESON

*School of Physics and Astronomy, University of Leeds LS2 9JT, UK*

*\*py12ej@leeds.ac.uk*

**Abstract:** An all-optical switchable twisted nematic liquid crystal system has been designed for use as a laser protection filter, which takes advantage of light-induced modification of liquid crystal order. The filter employs photochromic azo-doped liquid crystal mixtures that have been optically characterized and incorporated into a laser filter device. The ability to switch between transmission and blocking modes is shown to occur, even for incredibly low intensity (0.5 mW) irradiation with a continuous 405 nm laser. The blocking-state extinction is defined only by the polarizer extinction ratio, and sub-second switching is demonstrated for these low laser intensities. The response is sufficiently fast to provide protection for CCD cameras against laser damage. The optical switching time is shown to depend on both temperature and laser power. This automatic photo-switchable device offers an exciting approach for passive laser protection.

Published by The Optical Society under the terms of the [Creative Commons Attribution 4.0 License](#). Further on of this work must maintain attribution to the author(s) and the published article's title, journal citation, and DOI.

## 1. Introduction

The accessibility of high-powered hand-held lasers has led to an increase in accidental and malevolent exposure of cameras and eyes to high intensity radiation. Laser powers  $>5$  mW can potentially cause damage to eyesight or camera systems [1,2], with lower intensities still presenting a dazzle threat. There is therefore an increased urgency in providing optical solutions to this problem. To provide protection the device must be switchable, rapid, and have high optical densities. The use of liquid crystals (LC) in laser protection has been clearly demonstrated [3–5], with their electro-optical properties providing an excellent base for an electrically switchable filter. However, there is clear potential for using light-matter interactions in photochromic LCs to provide automatic, passive laser protection. Here, we demonstrate a new LC device that includes a photosensitive azo-LC as a passive all-optical switchable protection against continuous (CW) laser threats.

Photosensitive LCs are remarkable optical materials with a multitude of potential applications. Azobenzene-based mesogens, which may themselves exhibit LC phases [6,7], can be doped into LC systems allowing for manipulation of the material via external light stimuli. There has been considerable research on the behavior of chiral nematic LCs doped with azobenzene [8,9], azo-LC [10,11], and more recently azo-chiral dopants [12–16]. The combination of LCs and photosensitive azo-derivatives has led to a number of proposed applications including, but not limited to, photo-tuneable diffraction gratings [17,18], image-storage devices [14,19], and resonance tuning in plasmonic devices [20,21].

Azobenzene-based materials undergo a reversible trans-cis photoisomerisation when irradiated with wavelengths of light corresponding to the azo  $\pi$ - $\pi^*$  transition. This switch results in a conformational shape change, usually from rod-shaped to bent [Fig. 1(a)]. In LCs doped with azobenzene derivatives, the photoisomerisation of the dopant disrupts the host LC packing resulting in a light-induced reduction of order and overall change in the bulk material properties. For a high enough azo-dopant concentration, sufficient photo-switching may occur to induce an isothermal phase transition of the mixture. This isothermal phase transition effect, from nematic to isotropic, is utilised in this photoswitchable protection device.

LC devices have dominated the display industry for many years due to their exceptional electro-optic properties [22]. In this letter we are concerned with optically-induced switching, but still take advantage of key LC properties. Calamitic nematic LCs are formed from rod-like mesogens with the molecular long axis on average aligned in a preferred direction, denoted by the director  $\hat{n}$ . LCs exhibit a birefringence,  $\Delta n = n_{\parallel} - n_{\perp}$ , and when constrained between two planar aligned substrates, with rubbing directions at  $90^{\circ}$  to one another, a twisted nematic (TN) device is formed. In a TN device the LC director lies in the substrate plane and rotates by  $90^{\circ}$  through the sample, forming a helicoidal structure with a pitch  $P_0 = d/4$  ( $d$  is the cell gap). If a TN device is held between crossed polarisers waveguiding occurs for wavelengths of light below the Mauguin limit,  $\lambda \ll \Delta n P_0$ , rotating the input polarization by  $90^{\circ}$  allowing it to pass through the analyser. Neglecting optical losses of the complete system due to polarisers and Fresnel losses ( $\sim 55\%$  for unpolarised light), a TN device between crossed polarisers will transmit much of the incident white light. If the LC undergoes a phase transition to isotropic, the helicoidal structure and all birefringence is lost and the light is no longer transmitted. The light is thus effectively blocked, with the transmission purely determined by the polariser extinction ratio (PER). It is switching between these two modes, guiding and isotropic, that forms the basis of our device.

## 2. Materials and methods

Mixtures of 4-2-butyl-4'-2-alkoxyazobenzene [BAAB2, Fig. 1(a)], described further in [23], in 4-pentyl-4'-cyanobiphenyl (5CB) were created with varying concentration, between 5 and 10% (w/w), denoted mix-5 to mix-10. The mixtures were filled into  $\sim 3 \mu\text{m}$  cell gap TN devices (SE3510 polyimide alignment layers). BAAB2 itself has a nematic LC phase, so can be mixed with a nematic LC host such as 5CB without a solubility limit. Therefore, arbitrarily high concentrations could be used should specific device characteristics require them. The absorption spectrum for BAAB2 dissolved in acetone is shown in Fig. 1(b). The absorption peak at  $\lambda \sim 350 \text{ nm}$  corresponds to the azo  $\pi\text{-}\pi^*$  trans-cis transition, whilst the peak at  $\lambda \sim 432 \text{ nm}$  corresponds to the reverse cis-trans transition. Here, a low power laser (0.2-3.5 mW, beam diameter  $\sim 27 \text{ mm}$ ) of wavelength  $\lambda = 405 \text{ nm}$  was used to excite the azo transition and demonstrate the device. We were especially interested in the extent to which the filter could be tuned to protect even at very low, yet damaging/dazzling, laser powers.

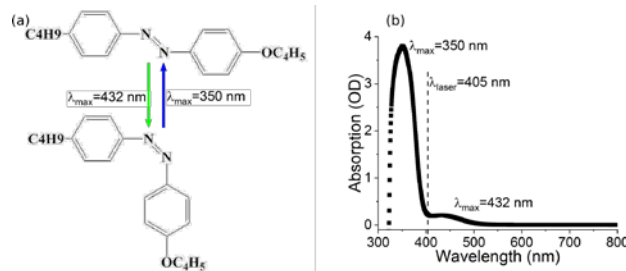


Fig. 1. (a) The structure and conformal shapes of BAAB2. (b) BAAB2 in acetone absorption spectrum, obtained using an Agilent UV/Vis 6000 spectrometer. All data can be found at <https://doi.org/10.5518/364>.

## 3. Results and discussion

The key to this filter is light-induced modification of the nematic to isotropic phase transition. Figure 2(a) summarises the nematic to isotropic phase transition temperature ( $T_{\text{NI}}$ ) measured under a variety of conditions for the mixtures. Differential scanning calorimetry (DSC,  $10^{\circ}\text{Cmin}^{-1}$ ) data demonstrates that  $T_{\text{NI}}$  increases with increasing concentration of BAAB2 dopant, as expected since BAAB2 has a higher  $T_{\text{NI}}$  than 5CB ( $T_{\text{NI}} = 83.5^{\circ}\text{C}$  and  $35.8^{\circ}\text{C}$

respectively). The same trends for  $T_{NI}$  are observed using white-light polarizing optical microscopy (POM,  $2\text{ }^{\circ}\text{Cmin}^{-1}$ ), coupled with a red filter to prevent the broadband light from photoisomerising the BAAB2 molecules; the  $1\text{ }^{\circ}\text{C}$  difference in the transition temperatures is attributable to the absolute accuracy of each measurement method ( $\pm 1\text{ }^{\circ}\text{C}$ ). The subsequent transition temperatures determined are compared with those from POM with the red filter as the relative accuracy in measurement of  $T_{NI}$  using the same method and hot stage is  $\pm 0.1\text{ }^{\circ}\text{C}$  and POM must be used to determine the optically-modified transition temperatures.

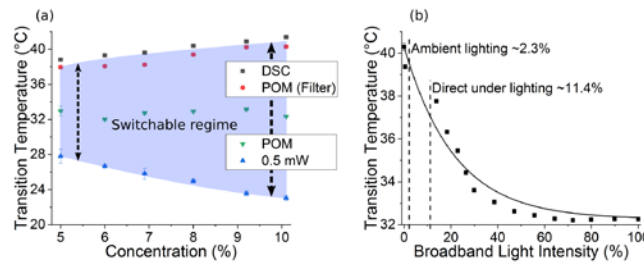


Fig. 2. (a)  $T_{NI}$  for dark and irradiated conditions using DSC and POM. (b) The variation in transition temperature under varying broadband intensity, compared with ambient intensity.

Without the red filter in place (illuminating with a broad-band white light spectrum),  $T_{NI}$  is observed to decrease due to the photoisomerisation occurring from the low wavelength contribution illuminating the sample. This decrease in  $T_{NI}$  would be observed in standard operation of the device and is therefore important to quantify. Our measurements indicate a reduction of  $\sim 7\text{ }^{\circ}\text{C}$  caused by white light from a 50 W halogen bulb in transmission focused onto the sample. The resulting photoisomerisation that occurs here is much larger than would be found in ambient room lighting, measured to be  $\sim 2.3\%$  the maximum microscope light intensity used. Figure 2(b) shows how the transition temperature for mix-10 (10% BAAB) varies with the percentage light intensity, compared with the maximum microscope intensity.

Investigations were carried out into the effect of CW laser irradiation (405 nm) on the  $T_{NI}$  for each mixture. The samples were irradiated with  $9.0\text{ mWcm}^{-2}$  (0.5 mW) for 5 minutes before measurements of the  $T_{NI}$  were conducted with continued irradiation. 5 minutes of irradiation is more than sufficient for the sample to equilibrate, hence ensuring reproducibility. The photoisomerisation of BAAB2 causes a large reduction ( $\sim 10\text{ }^{\circ}\text{C}$ ) in  $T_{NI}$ . The transition temperature of mixtures under irradiation ( $T_{Irr-NI}$ ) decreases with increasing BAAB2 concentration due to the increased amount of conformational change occurring in the sample. The temperature regime between  $T_{NI}$  and  $T_{Irr-NI}$  is denoted the switchable protection regime of this device. Between these temperatures, if the system is exposed to laser radiation, in this case a low intensity of 0.5 mW, it will undergo an isothermal phase transition from nematic to isotropic, thus taking the device from transmitting (TN configuration, waveguiding between crossed polarisers) to blocking (isotropic and hence dark between crossed polarisers). This protection regime could be readily tuned to a specified temperature range by altering the LC host, or azo-LC dopant concentration.

To fully assess the optical properties of the mixtures, the wavelength dispersion of the birefringence was determined; this was measured for each mixture and compared with 5CB at  $T = 25\text{ }^{\circ}\text{C}$  [Fig. 3(a)] using quasi-monochromatic illumination. The mixtures have a greater birefringence than 5CB, and fitting the extended Cauchy model [24] reveals that the mean resonance wavelength,  $\lambda^*$ , corresponding to the  $\pi$ - $\pi^*$  transition, increases for BAAB2 doped 5CB. This is a result of the higher wavelength absorption peak of BAAB2 at  $\lambda^* = 350\text{ nm}$ , compared with 5CB where  $\lambda^* = 210\text{ nm}$  [25].

When the device is held between  $T_{NI}$  and  $T_{Irr-NI}$  (switchable protection regime) the device will switch between transmitting and blocking modes when it is exposed to irradiation of the laser “threat”. In Fig. 3(b) the transmission (pre-irradiation) and blocking state (post-

irradiation) spectra for mix-10 are shown. The spectra and inserts demonstrate the ability for effective observations across the visible spectrum whilst in the transmission mode. After irradiation with the “threat” laser wavelength the transmission drops to zero, with the transmission blocked by the crossed polarisers to a degree determined purely by their extinction ratio. Once the “threat” is removed the azo-dopant thermally relaxes into the trans-state, transmission mode, typically within 1 hour, depending on the device temperature.

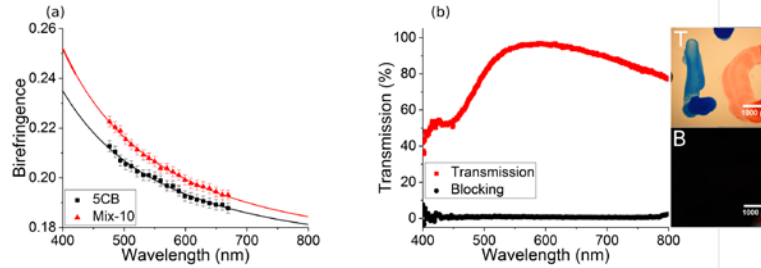


Fig. 3. (a) The experimental wavelength dispersion measurements of 5CB and mix-10. Solid lines show the extended Cauchy model fit (parameters:  $S_{5CB} = 0.67$ ,  $\lambda_{5CB}^* = 223$  nm,  $G_{5CB} = 3.4$ ,  $S_{mix-10} = 0.60$ ,  $\lambda_{mix-10}^* = 243$  nm, and  $G_{mix-10} = 3.1$ ). (b) Transmission and blocking spectra for mix-10. Inserts show imaging through the device, captured using a Nikon D7100 camera.

An important aspect of switchable laser protection lies in the response speed of the device. The transmission through the device was measured using a photodiode and the response time from the point of first irradiation to 10% transmission was evaluated; this is chosen as it gives a robust comparison between different experimental conditions, as well as being a common standard in LC response time measurements. BAAB2 concentration, temperature, and laser power will all effect the response time and here each is evaluated in turn.

The response time was measured for temperatures across each mixture’s protection regime following laser irradiation with  $9.0 \text{ mWcm}^{-2}$  ( $0.5 \text{ mW}$ ). Figure 4(a) demonstrates the response time variation with temperature for mix-5 and mix-10. The increased operational temperature range of mix-10 is clear. By plotting the response time as a function of reduced temperature ( $T_{NI} - T$ ), Fig. 4(b), we can clearly see the response time of the mixtures increases when cooling from  $T_{NI}$ . Interestingly, the response times for samples held within a few degrees of  $T_{NI}$  are as fast as only a few hundred milliseconds, even for this incredibly low laser intensity.

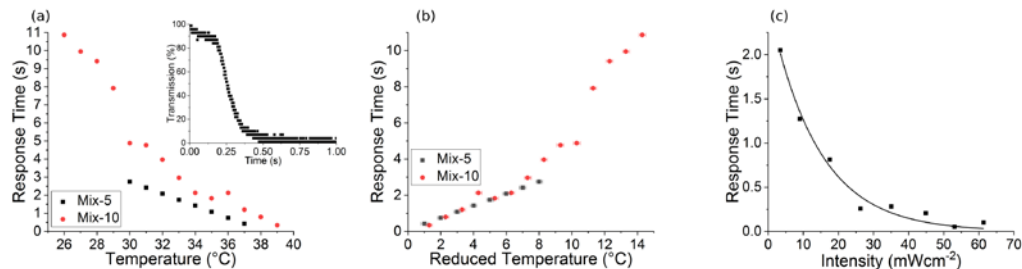


Fig. 4. Response time dependence on (a) temperature, (b) reduced temperature (for mix-5 and mix-10), and (c) laser intensity (for mix-10, at  $T = 38$  °C). Insert demonstrates typical transmission response.

The laser intensity irradiating the system will also impact the response time of the system. Figure 4(c) show the rapid decrease of the response time for mix-10, at  $2$  °C below  $T_{NI}$ , with increasing laser intensity. Higher laser intensities are known to result in an increased rate of photo-switching of azo-LC and therefore a faster response time [26]. This means that if the system was “under threat” from higher-powered lasers it would result in a reduced exposure

time, and therefore higher levels of protection. In our case, irradiation of the device by higher laser intensities achieved an incredibly rapid photo-induced response time of 51 ms. It is also important to consider how the laser wavelength and azo-LC absorption bands overlap. In this case the laser wavelength, 405nm, was right at the edge of the absorption band, and the small absorption at this wavelength [Fig. 1(b)] has the effect of reducing the possible response time of the system. The closer the irradiating wavelength is to the peak of the absorption band, the faster the response time of the system, something easily achieved through careful consideration of dopant and device design.

When considering the protection provided by a laser filter device for CCD cameras, or otherwise, the response time of the system is of paramount importance. When the response times measured here are compared with literature describing the damage to colour CCD cameras from CW laser radiation the protection provided by this all-optical switchable device can be evaluated [27]. This literature states that a colour CCD camera experiences damage from laser intensities of  $16 \text{ kWcm}^{-2}$ , much larger than our maximum intensity used of  $61.3 \text{ mWcm}^{-2}$ , after exposure times of greater than 1 s. If we consider the response time measured here, Fig. 4, we have shown switching speeds considerably less than 1 s, with much lower laser intensities. This clearly demonstrates that the passive all-optical switchable protection device will provide protection against damage for colour CCD cameras against large laser intensities and thus also protect against the dazzle threat of much lower power lasers. It is important to emphasize that the response time shown here was measured with an incredibly low laser intensity of  $9.0 \text{ mWcm}^{-2}$ , approximately  $10^6$  times smaller than the indicated damage threshold of  $16 \text{ kWcm}^{-2}$ . As demonstrated in Fig. 4(c) the response time reduces rapidly with increasing laser intensity and therefore the switching speed measured would decrease, providing an even faster response time and therefore greater protection.

#### 4. Conclusion

An all-optical switchable laser protection filter has been demonstrated. The optical properties of an azo-LC doped LC system have been characterized and accurate fitting of the wavelength dispersion was undertaken. The ability of the device to switch rapidly between a transmitting and blocking mode via irradiation by a laser “threat” has been demonstrated. The transmission mode provides an excellent image with little colour distortion. Conversely, the blocking state of the device has a transmission limited purely by the PER. The ability of the system to provide protection from different laser wavelengths is also possible by doping the LC host with a suitable azo dopant with the structure altered such that the  $\pi$ - $\pi^*$  absorption band matches the laser “threat”.

The response speed of this all-optical device was thoroughly investigated and shown to depend on the temperature and laser intensity, with a rapid response of 51 ms demonstrated. It has been clearly shown that the device would provide protection against large CW laser intensities for CCD cameras. The implementation of the protection system would be incredibly simple, with no requirement for sensor detection of threat or voltage application. Thus, this azo-doped LC system has been shown to be an effective passive solution to the threat from laser irradiation.

#### Funding

Engineering and Physical Sciences Research Council (EP/N509681/1).

#### Acknowledgments

The photo-switchable materials were provided through a collaboration with S. V. Serak and V. A. Grozhik, funded through INTAS-BELARUS N97-0635 (2001). The authors are grateful for the continued use of these interesting photochromic materials.

## References

1. M. D. Harris, A. E. Lincoln, P. J. Amoroso, B. Stuck, and D. Sliney, "Laser eye injuries in military occupations," *Aviat. Space Environ. Med.* **74**(9), 947–952 (2003).
2. American National Standard (2014). American National Standard for Safe Use of Lasers. [Online]. Florida: Laser Institute of America. [29th June 18.] Available from: [www.lia.org](http://www.lia.org)
3. E. I. L. Jull and H. F. Gleeson, "Tuneable and switchable liquid crystal laser protection system," *Appl. Opt.* **56**(29), 8061–8066 (2017).
4. A. Rees and J. Staromlynska, "Automatic laser light detection and filtering using a liquid crystal Lyot filter," *J. Nonlinear Opt. Phys.* **2**(04), 661–676 (1993).
5. C. S. Wu and S. T. Wu, "Liquid-crystal-based switchable polarizers for sensor protection," *Appl. Opt.* **34**(31), 7221–7227 (1995).
6. U. Hrozhyk, S. Serak, N. Tabiryman, and T. J. Bunning, "Wide temperature range azobenzene nematic and smectic LC materials," *Mol. Cryst. Liq. Cryst.* **454**, 235–245 (2006).
7. C. Selvarasu and P. Kannan, "Effect of azo and ester linkages on rod shaped Schiff base liquid crystals and their photophysical investigations," *J. Mol. Struct.* **1125**, 234–240 (2016).
8. H. Lee, K. Doi, H. Harada, O. Tsutsumi, A. Kanazawa, T. Shiono, and T. Ikeda, "Photochemical modulation of color and transmittance in chiral nematic liquid crystal containing an azobenzene as a photosensitive chromophore," *J. Phys. Chem. B* **104**(30), 7023–7028 (2000).
9. U. A. Hrozhyk, S. V. Serak, N. V. Tabiryman, T. J. White, and T. J. Bunning, "Optically switchable, rapidly relaxing cholesteric liquid crystal reflectors," *Opt. Express* **18**(9), 9651–9657 (2010).
10. U. A. Hrozhyk, S. V. Serak, N. V. Tabiryman, and T. J. Bunning, "Optical tuning of the reflection of cholesterics doped with azobenzene liquid crystals," *Adv. Funct. Mater.* **17**(11), 1735–1742 (2007).
11. J. D. Lin, Y. M. Lin, T. S. Mo, and C. R. Lee, "Photosensitive and all-optically fast-controllable photonic bandgap device and laser in a dye-doped blue phase with a low-concentration azobenzene liquid crystal," *Opt. Express* **22**(8), 9171–9181 (2014).
12. N. Venkataraman, G. Magyar, M. Lightfoot, E. Montbach, A. Khan, T. Schneider, J. W. Doane, L. Green, and Q. Li, "Thin flexible photosensitive cholesteric displays," *J. SID.* **17**(10), 869–873 (2009).
13. T. V. Mykytiuk, I. P. Ilchishin, O. V. Yaroshchuk, R. M. Kravchuk, Y. Li, and Q. Li, "Rapid reversible phototuning of lasing frequency in dye-doped cholesteric liquid crystal," *Opt. Lett.* **39**(22), 6490–6493 (2014).
14. S. Chen, Y. Chen, X. Tong, B. Wu, M. Ma, Y. Shi, and X. Wang, "Room temperature optical image storage devices based on novel photo-responsive chiral azobenzene liquid crystal dopants," *Mater. Res. Express* **3**(11), 115701 (2016).
15. P. V. Dolganov, S. O. Gordeev, V. K. Dolganov, and A. Yu. Bobrovsky, "Photo- and thermo-induced variation of photonic properties of cholesteric liquid crystal containing azobenzene-based chiral dopant," *Mol. Cryst. Liq. Cryst. (Phila. Pa.)* **633**(1), 14–22 (2016).
16. Y. C. Hsiao, K. C. Huang, and W. Lee, "Photo-switchable chiral liquid crystal with optical tristability enabled by a photoresponsive azo-chiral dopant," *Opt. Express* **25**(3), 2687–2693 (2017).
17. L. DeSio, S. Serak, N. Tabiryman, and C. Umeton, "Mesogenic versus non-mesogenic azo dye confined in a soft-matter template for realization of optically switchable diffraction gratings," *J. Mater. Chem.* **21**(19), 6811–6814 (2011).
18. L. de Sio, L. Ricciardi, S. Serak, M. La Deda, N. Tabiryman, and C. Umeton, "Photo-sensitive liquid crystals for optically controlled diffraction gratings," *J. Mater. Chem.* **22**(14), 6669–6673 (2012).
19. T. Ikeda and O. Tsutsumi, "Optical switching and image storage by means of azobenzene liquid-crystal films," *Science* **268**(5219), 1873–1875 (1995).
20. Z. Chen, V. K. S. Hsiao, X. Li, Z. Li, J. Yu, and J. Zhang, "Optically tunable microfiber-knot resonator," *Opt. Express* **19**(15), 14217–14222 (2011).
21. G. Gilardi, S. Xiao, N. Asger Mortensen, A. d' Alessandro, and R. Beccherelli, "Plasmon resonance optical tuning based on photosensitive composite structures," *J. Opt. Soc. Am. B* **31**(2), 360–365 (2014).
22. J. W. Goodby, P. J. Collings, K. Takashi, C. Tschierske, H. F. Gleeson, and P. Raynes, *Handbook of Liquid Crystals Volume 8: Applications of Liquid Crystals* (Wiley, 2014) 2nd Edition.
23. S. V. Serak, E. O. Arikainen, H. F. Gleeson, V. A. Grozhik, J. P. Guillou, and N. A. Usova, "Laser-induced concentric colour domains in a cholesteric liquid crystal mixture containing a nematic azobenzene dopant," *Liq. Cryst.* **29**(1), 19–26 (2002).
24. J. Li and S. Wu, "Extended Cauchy equations for the refractive indices of liquid crystals," *J. Appl. Phys.* **95**(3), 896–901 (2004).
25. J. Li, *Refractive indices of liquid crystals and their applications in display and photonic devices*, doctoral dissertation, university of central Florida. (2005).
26. I. C. Khoo, M. Wood, M. Y. Shih, and P. Chen, "Extremely nonlinear photosensitive liquid crystals for image sensing and sensor protection," *Opt. Express* **4**(11), 432–442 (1999).
27. B. Schwarz, G. Ritt, M. Koerber, and B. Eberle, "Laser-induced damage threshold of camera sensors and micro-optoelectromechanical systems," *Opt. Eng.* **56**(3), 034108 (2017).